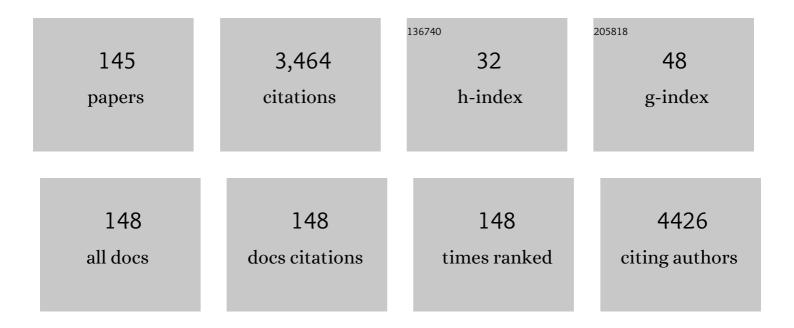
Koji Kamagata

List of Publications by Year in descending order

Source: https://exaly.com/author-pdf/13526/publications.pdf Version: 2024-02-01



#	Article	IF	CITATIONS
1	Simultaneous relaxometry and morphometry of human brain structures with 3D magnetic resonance fingerprinting: a multicenter, multiplatform, multifield-strength study. Cerebral Cortex, 2023, 33, 729-739.	1.6	4
2	Role of right temporoparietal junction for counterfactual evaluation of partner's decision in ultimatum game. Cerebral Cortex, 2023, 33, 2947-2957.	1.6	5
3	Reproducibility of diffusion tensor image analysis along the perivascular space (DTI-ALPS) for evaluating interstitial fluid diffusivity and glymphatic function: CHanges in Alps index on Multiple conditiON acqulsition eXperiment (CHAMONIX) study. Japanese Journal of Radiology, 2022, 40, 147-158.	1.0	87
4	Multiple sclerosis plaques may undergo continuous myelin degradation: a cross-sectional study with myelin and axon-related quantitative magnetic resonance imaging metrics. Neuroradiology, 2022, 64, 465-471.	1.1	4
5	An Investigation of Water Diffusivity Changes along the Perivascular Space in Elderly Subjects with Hypertension. American Journal of Neuroradiology, 2022, 43, 48-55.	1.2	28
6	Development of a Deep Learning Algorithm to Generate MR Angiography from 3D Quantitative Synthetic MR Imaging [Proceedings of the 2019 Young Investigator Award]. Japanese Journal of Magnetic Resonance in Medicine, 2022, 42, .	0.0	0
7	White matter microstructures in Parkinson's disease with and without impulse control behaviors. Annals of Clinical and Translational Neurology, 2022, , .	1.7	6
8	Diffusion magnetic resonance tractography-based evaluation of commissural fiber abnormalities in a heparan sulfate endosulfatase-deficient mouse brain. Magnetic Resonance Imaging, 2022, 88, 123-123.	1.0	0
9	Advantages of Using Both Voxel- and Surface-based Morphometry in Cortical Morphology Analysis: A Review of Various Applications. Magnetic Resonance in Medical Sciences, 2022, 21, 41-57.	1.1	31
10	Advanced Diffusion MR Imaging for Multiple Sclerosis in the Brain and Spinal Cord. Magnetic Resonance in Medical Sciences, 2022, 21, 58-70.	1.1	9
11	Effect of Temporal Sampling Rate on Estimates of the Perfusion Parameters for Patients with Moyamoya Disease Assessed with Simultaneous Multislice Dynamic Susceptibility Contrast-enhanced MR Imaging. Magnetic Resonance in Medical Sciences, 2022, , .	1.1	0
12	Analysis of synthetic magnetic resonance images by multi-channel segmentation increases accuracy of volumetry in the putamen and decreases mis-segmentation in the dural sinuses. Acta Radiologica, 2022, , 028418512210898.	0.5	0
13	Radiomics with 3-dimensional magnetic resonance fingerprinting: influence of dictionary design on repeatability and reproducibility of radiomic features. European Radiology, 2022, 32, 4791-4800.	2.3	4
14	Multimodal magnetic resonance imaging quantification of gray matter alterations in relapsingâ€remitting multiple sclerosis and neuromyelitis optica spectrum disorder. Journal of Neuroscience Research, 2022, 100, 1395-1412.	1.3	3
15	Size-reweighted cascaded fully convolutional network for substantia nigra segmentation from T2 MRI. , 2022, , .		0
16	Substantia nigra analysis by tensor decomposition of T2-weighted images for Parkinson's disease diagnosis. , 2022, , .		0
17	Rigid real-time prospective motion-corrected three-dimensional multiparametric mapping of the human brain. NeuroImage, 2022, 255, 119176.	2.1	5
18	Microstructural white matter abnormalities in multiple sclerosis and neuromyelitis optica spectrum disorders: Evaluation by advanced diffusion imaging. Journal of the Neurological Sciences, 2022, 436, 120205.	0.3	12

#	Article	IF	CITATIONS
19	Network Centrality Analysis Characterizes Brain Activity during Response Inhibition in Right Ventral Inferior Frontal Cortex. Juntendo Medical Journal, 2022, 68, 208-211.	0.1	3
20	White matter fiber-specific degeneration in older adults with metabolic syndrome. Molecular Metabolism, 2022, 62, 101527.	3.0	7
21	Influence of Mild White Matter Lesions on Voxel-based Morphometry. Magnetic Resonance in Medical Sciences, 2021, 20, 40-46.	1.1	3
22	Repeatability and reproducibility of human brain morphometry using threeâ€dimensional magnetic resonance fingerprinting. Human Brain Mapping, 2021, 42, 275-285.	1.9	13
23	Parkinson's disease: deep learning with a parameter-weighted structural connectome matrix for diagnosis and neural circuit disorder investigation. Neuroradiology, 2021, 63, 1451-1462.	1.1	22
24	Neuronuclear and Neuromelaninâ€6ensitive Imaging for Acquired Hepatocerebral Degeneration with Parkinsonism. Movement Disorders Clinical Practice, 2021, 8, 464-468.	0.8	0
25	Possible Neuroprotective Effects of l-Carnitine on White-Matter Microstructural Damage and Cognitive Decline in Hemodialysis Patients. Nutrients, 2021, 13, 1292.	1.7	4
26	Effect of hybrid of compressed sensing and parallel imaging on the quantitative values measured by 3D quantitative synthetic MRI: A phantom study. Magnetic Resonance Imaging, 2021, 78, 90-97.	1.0	6
27	Differentiation between multiple sclerosis and neuromyelitis optica spectrum disorders by multiparametric quantitative MRI using convolutional neural network. Journal of Clinical Neuroscience, 2021, 87, 55-58.	0.8	8
28	Diffusion Magnetic Resonance Imaging-Based Biomarkers for Neurodegenerative Diseases. International Journal of Molecular Sciences, 2021, 22, 5216.	1.8	39
29	Neurite orientation dispersion and density imaging reveals white matter microstructural alterations in adults with autism. Molecular Autism, 2021, 12, 48.	2.6	17
30	Fiber-specific white matter alterations in early-stage tremor-dominant Parkinson's disease. Npj Parkinson's Disease, 2021, 7, 51.	2,5	9
31	Connectome analysis of male world lass gymnasts using probabilistic multishell, multitissue constrained spherical deconvolution tracking. Journal of Neuroscience Research, 2021, 99, 2558-2572.	1.3	1
32	Diffusion MRI Captures White Matter Microstructure Alterations in PRKN Disease. Journal of Parkinson's Disease, 2021, 11, 1221-1235.	1.5	1
33	White matter alterations in Parkinson's disease with levodopa-induced dyskinesia. Parkinsonism and Related Disorders, 2021, 90, 8-14.	1.1	9
34	Parallel cognitive processing streams in human prefrontal cortex: Parsing areal-level brain network for response inhibition. Cell Reports, 2021, 36, 109732.	2.9	15
35	3D Quantitative Synthetic MRI in the Evaluation of Multiple Sclerosis Lesions. American Journal of Neuroradiology, 2021, 42, 471-478.	1.2	16
36	Age-Related Changes in Relaxation Times, Proton Density, Myelin, and Tissue Volumes in Adult Brain Analyzed by 2-Dimensional Quantitative Synthetic Magnetic Resonance Imaging. Investigative Radiology, 2021, 56, 163-172.	3.5	30

#	Article	IF	CITATIONS
37	Cross-scanner reproducibility and harmonization of a diffusion MRI structural brain network: A traveling subject study of multi-b acquisition. NeuroImage, 2021, 245, 118675.	2.1	15
38	White matter and nigral alterations in multiple system atrophy-parkinsonian type. Npj Parkinson's Disease, 2021, 7, 96.	2.5	10
39	Accelerated Isotropic Multiparametric Imaging by High Spatial Resolution 3D-QALAS With Compressed Sensing. Investigative Radiology, 2021, 56, 292-300.	3.5	23
40	Automation of a Rule-based Workflow to Estimate Age from Brain MR Imaging of Infants and Children Up to 2 Years Old Using Stacked Deep Learning. Magnetic Resonance in Medical Sciences, 2021, , .	1.1	5
41	Ventricular volumetry and free-water corrected diffusion tensor imaging of the anterior thalamic radiation in idiopathic normal pressure hydrocephalus. Journal of Neuroradiology, 2020, 47, 312-317.	0.6	10
42	Evaluation of white matter microstructure in patients with Parkinson's disease using microscopic fractional anisotropy. Neuroradiology, 2020, 62, 197-203.	1.1	7
43	Effect of changing the analyzed image contrast on the accuracy of intracranial volume extraction using Brain Extraction Tool 2. Radiological Physics and Technology, 2020, 13, 76-82.	1.0	4
44	Scan–rescan and inter-vendor reproducibility of neurite orientation dispersion and density imaging metrics. Neuroradiology, 2020, 62, 483-494.	1.1	26
45	MR Biomarkers of Degenerative Brain Disorders Derived From Diffusion Imaging. Journal of Magnetic Resonance Imaging, 2020, 52, 1620-1636.	1.9	75
46	Connectivity-based localization of human hypothalamic nuclei in functional images of standard voxel size. Neurolmage, 2020, 221, 117205.	2.1	9
47	Functional Organization for Response Inhibition in the Right Inferior Frontal Cortex of Individual Human Brains. Cerebral Cortex, 2020, 30, 6325-6335.	1.6	28
48	Brain White-Matter Degeneration Due to Aging and Parkinson Disease as Revealed by Double Diffusion Encoding. Frontiers in Neuroscience, 2020, 14, 584510.	1.4	18
49	Regional brain gray matter volume in world-class artistic gymnasts. Journal of Physiological Sciences, 2020, 70, 43.	0.9	5
50	Leigh Syndrome Due to NDUFV1 Mutations Initially Presenting as LBSL. Genes, 2020, 11, 1325.	1.0	8
51	Deep Learning Approach for Generating MRA Images From 3D Quantitative Synthetic MRI Without Additional Scans. Investigative Radiology, 2020, 55, 249-256.	3.5	34
52	Network Centrality Reveals Dissociable Brain Activity during Response Inhibition in Human Right Ventral Part of Inferior Frontal Cortex. Neuroscience, 2020, 433, 163-173.	1.1	16
53	Deep Learning for MR Angiography Synthesis using 3D Quantitative Synthetic MR Imaging [Presidential Award Proceedings]. Japanese Journal of Magnetic Resonance in Medicine, 2020, 40, 20-23.	0.0	0
54	Differentiation of high-grade and low-grade intra-axial brain tumors by time-dependent diffusion MRI. Magnetic Resonance Imaging, 2020, 72, 34-41.	1.0	22

#	Article	IF	CITATIONS
55	Dissociable Networks of the Lateral/Medial Mammillary Body in the Human Brain. Frontiers in Human Neuroscience, 2020, 14, 228.	1.0	7
56	Image Domain Transfer by Deep Learning is Feasible in Multiple Sclerosis Clinical Practice. Investigative Radiology, 2020, 55, 324-325.	3.5	3
57	A Novel Deep Learning Approach with a 3D Convolutional Ladder Network for Differential Diagnosis of Idiopathic Normal Pressure Hydrocephalus and Alzheimer's Disease. Magnetic Resonance in Medical Sciences, 2020, 19, 351-358.	1.1	23
58	Neurocognitive and psychiatric disordersâ€related axonal degeneration in Parkinson's disease. Journal of Neuroscience Research, 2020, 98, 936-949.	1.3	15
59	Measured volumes using segmented tissue probability data obtained using statistical parametric mapping 12 were not influenced by the contrasts of analyzed images. Journal of Clinical Neuroscience, 2020, 74, 69-75.	0.8	Ο
60	Myelin Measurement Using Quantitative Magnetic Resonance Imaging: A Correlation Study Comparing Various Imaging Techniques in Patients with Multiple Sclerosis. Cells, 2020, 9, 393.	1.8	28
61	Neuroimaging evaluation and successful treatment by using directional deep brain stimulation and levodopa in a patient with GNAO1-associated movement disorder: A case report. Journal of the Neurological Sciences, 2020, 411, 116710.	0.3	15
62	Estimation of intracranial volume: A comparative study between synthetic MRI and FSL-brain extraction tool (BET)2. Journal of Clinical Neuroscience, 2020, 79, 178-182.	0.8	8
63	Advanced diffusion magnetic resonance imaging in patients with Alzheimer's and Parkinson's diseases. Neural Regeneration Research, 2020, 15, 1590.	1.6	28
64	White Matter Myelin Changes Related to Long-term Intensive Training in Japanese World-class Gymnasts. Juntendo Medical Journal, 2020, 66, 21-28.	0.1	0
65	Lesion Detection of Cerebral Infarction by a Machine Learning Model that Learned â€~Normal' [Presidential Award Proceedings]. Japanese Journal of Magnetic Resonance in Medicine, 2020, 40, 26-29.	0.0	Ο
66	Free-Water Imaging in White and Gray Matter in Parkinson's Disease. Cells, 2019, 8, 839.	1.8	44
67	Convolutional neural network-based segmentation can help in assessing the substantia nigra in neuromelanin MRI. Neuroradiology, 2019, 61, 1387-1395.	1.1	36
68	Aberrant myelination in patients with Sturge-Weber syndrome analyzed using synthetic quantitative magnetic resonance imaging. Neuroradiology, 2019, 61, 1055-1066.	1.1	17
69	MRI-based visualization of rTMS-induced cortical plasticity in the primary motor cortex. PLoS ONE, 2019, 14, e0224175.	1.1	16
70	Three-dimensional high-resolution simultaneous quantitative mapping of the whole brain with 3D-QALAS: An accuracy and repeatability study. Magnetic Resonance Imaging, 2019, 63, 235-243.	1.0	46
71	White Matter Abnormalities in Multiple Sclerosis Evaluated by Quantitative Synthetic MRI, Diffusion Tensor Imaging, and Neurite Orientation Dispersion and Density Imaging. American Journal of Neuroradiology, 2019, 40, 1642-1648.	1.2	33
72	MR g-ratio-weighted connectome analysis in patients with multiple sclerosis. Scientific Reports, 2019, 9, 13522.	1.6	27

#	Article	IF	CITATIONS
73	An Essential Role of the Intraparietal Sulcus in Response Inhibition Predicted by Parcellation-Based Network. Journal of Neuroscience, 2019, 39, 2509-2521.	1.7	59
74	Improving the Quality of Synthetic FLAIR Images with Deep Learning Using a Conditional Generative Adversarial Network for Pixel-by-Pixel Image Translation. American Journal of Neuroradiology, 2019, 40, 224-230.	1.2	59
75	Brain tissue and myelin volumetric analysis in multiple sclerosis at 3T MRI with various in-plane resolutions using synthetic MRI. Neuroradiology, 2019, 61, 1219-1227.	1.1	21
76	Comparison of magnetization transfer contrast of conventional and simultaneous multislice turbo spin echo acquisitions focusing on excitation time interval. Japanese Journal of Radiology, 2019, 37, 579-589.	1.0	1
77	White matter alterations in adult with autism spectrum disorder evaluated using diffusion kurtosis imaging. Neuroradiology, 2019, 61, 1343-1353.	1.1	13
78	Neuromelanin or DaTâ€ <scp>SPECT</scp> : which is the better marker for discriminating advanced Parkinson's disease?. European Journal of Neurology, 2019, 26, 1408-1416.	1.7	28
79	A metabolic profile of polyamines in parkinson disease: A promising biomarker. Annals of Neurology, 2019, 86, 251-263.	2.8	74
80	Gray Matter Alterations in Early and Late Relapsing-Remitting Multiple Sclerosis Evaluated with Synthetic Quantitative Magnetic Resonance Imaging. Scientific Reports, 2019, 9, 8147.	1.6	16
81	3D quantitative synthetic MRIâ€derived cortical thickness and subcortical brain volumes: Scan–rescan repeatability and comparison with conventional T ₁ â€weighted images. Journal of Magnetic Resonance Imaging, 2019, 50, 1834-1842.	1.9	37
82	Large hospital variation in the utilization of Post-procedural CT to detect pulmonary embolism/Deep Vein Thrombosis in Patients Undergoing Total Knee or Hip Replacement Surgery: Japanese Nationwide Diagnosis Procedure Combination Database Study. British Journal of Radiology, 2019, 92, 20180825.	1.0	3
83	Review of synthetic MRI in pediatric brains: Basic principle of MR quantification, its features, clinical applications, and limitations. Journal of Neuroradiology, 2019, 46, 268-275.	0.6	39
84	A Comparison of Techniques for Correcting Eddy-current and Motion-induced Distortions in Diffusion-weighted Echo-planar Images. Magnetic Resonance in Medical Sciences, 2019, 18, 272-275.	1.1	2
85	Linearity, Bias, Intrascanner Repeatability, and Interscanner Reproducibility of Quantitative Multidynamic Multiecho Sequence for Rapid Simultaneous Relaxometry at 3 T. Investigative Radiology, 2019, 54, 39-47.	3.5	79
86	Choroid plexus cysts analyzed using diffusion-weighted imaging with short diffusion-time. Magnetic Resonance Imaging, 2019, 57, 323-327.	1.0	16
87	Effect of Gadolinium on the Estimation of Myelin and Brain Tissue Volumes Based on Quantitative Synthetic MRI. American Journal of Neuroradiology, 2019, 40, 231-237.	1.2	9
88	Differentiating Alzheimer's Disease from Dementia with Lewy Bodies Using a Deep Learning Technique Based on Structural Brain Connectivity. Magnetic Resonance in Medical Sciences, 2019, 18, 219-224.	1.1	25
89	Dopamine transporter imaging predicts motor responsiveness to levodopa challenge in patients with Parkinson's disease: A pilot study of DATSCAN for subthalamic deep brain stimulation. Journal of the Neurological Sciences, 2018, 385, 134-139.	0.3	7
90	Automated brain tissue and myelin volumetry based on quantitative MR imaging with various in-plane resolutions. Journal of Neuroradiology, 2018, 45, 164-168.	0.6	33

#	Article	IF	CITATIONS
91	Changes in the ADC of diffusion-weighted MRI with the oscillating gradient spin-echo (OGSE) sequence due to differences in substrate viscosities. Japanese Journal of Radiology, 2018, 36, 415-420.	1.0	13
92	Application of Quantitative Microstructural MR Imaging with Atlas-based Analysis for the Spinal Cord in Cervical Spondylotic Myelopathy. Scientific Reports, 2018, 8, 5213.	1.6	28
93	Neurite orientation dispersion and density imaging of the nigrostriatal pathway in Parkinson's disease: Retrograde degeneration observed by tract-profile analysis. Parkinsonism and Related Disorders, 2018, 51, 55-60.	1.1	47
94	Depressive symptoms in Parkinson's disease are related to decreased left hippocampal volume: correlation with the 15-item shortened version of the Geriatric Depression Scale. Acta Radiologica, 2018, 59, 341-345.	0.5	18
95	Slice-accelerated gradient-echo echo planar imaging dynamic susceptibility contrast-enhanced MRI with blipped CAIPI: effect of increasing temporal resolution. Japanese Journal of Radiology, 2018, 36, 40-50.	1.0	3
96	Radiologist involvement is associated with reduced use of MRI in the acute period of low back pain in a non-elderly population. European Radiology, 2018, 28, 1600-1608.	2.3	3
97	Connectome analysis with diffusion MRI in idiopathic Parkinson's disease: Evaluation using multi-shell, multi-tissue, constrained spherical deconvolution. NeuroImage: Clinical, 2018, 17, 518-529.	1.4	51
98	Spatial Restriction within Intracranial Epidermoid Cysts Observed Using Short Diffusion-time Diffusion-weighted Imaging. Magnetic Resonance in Medical Sciences, 2018, 17, 269-272.	1.1	24
99	Combining Segmented Grey and White Matter Images Improves Voxel-based Morphometry for the Case of Dilated Lateral Ventricles. Magnetic Resonance in Medical Sciences, 2018, 17, 293-300.	1.1	10
100	The Relationship between Neurite Density Measured with Confocal Microscopy in a Cleared Mouse Brain and Metrics Obtained from Diffusion Tensor and Diffusion Kurtosis Imaging. Magnetic Resonance in Medical Sciences, 2018, 17, 138-144.	1.1	12
101	Neuromelanin imaging and midbrain volumetry in progressive supranuclear palsy and Parkinson's disease. Movement Disorders, 2018, 33, 1488-1492.	2.2	39
102	The Advantage of Synthetic MRI for the Visualization of Anterior Temporal Pole Lesions on Double Inversion Recovery (DIR), Phase-sensitive Inversion Recovery (PSIR), and Myelin Images in a Patient with CADASIL. Magnetic Resonance in Medical Sciences, 2018, 17, 275-276.	1.1	24
103	Myelin Measurement: Comparison Between Simultaneous Tissue Relaxometry, Magnetization Transfer Saturation Index, and T1w/T2w Ratio Methods. Scientific Reports, 2018, 8, 10554.	1.6	91
104	Alterations of the optic pathway between unilateral and bilateral optic nerve damage in multiple sclerosis as revealed by the combined use of advanced diffusion kurtosis imaging and visual evoked potentials. Magnetic Resonance Imaging, 2017, 39, 24-30.	1.0	19
105	Neuromelanin MRI is useful for monitoring motor complications in Parkinson's and PARK2 disease. Journal of Neural Transmission, 2017, 124, 407-415.	1.4	31
106	Gray Matter Abnormalities in Idiopathic <scp>P</scp> arkinson's Disease: Evaluation by Diffusional Kurtosis Imaging and Neurite Orientation Dispersion and Density Imaging. Human Brain Mapping, 2017, 38, 3704-3722.	1.9	78
107	Diffusion imaging of reversible and irreversible microstructural changes within the corticospinal tract in idiopathic normal pressure hydrocephalus. NeuroImage: Clinical, 2017, 14, 663-671.	1.4	42
108	Usefulness of Non–Contrast-Enhanced MR Angiography Using a Silent Scan for Follow-Up after Y-Configuration Stent-Assisted Coil Embolization for Basilar Tip Aneurysms. American Journal of Neuroradiology, 2017, 38, 577-581.	1.2	44

#	Article	IF	CITATIONS
109	Diagnostic imaging of dementia with Lewy bodies by susceptibility-weighted imaging of nigrosomes versus striatal dopamine transporter single-photon emission computed tomography: a retrospective observational study. Neuroradiology, 2017, 59, 89-98.	1.1	28
110	Synthetic MRI in the Detection of Multiple Sclerosis Plaques. American Journal of Neuroradiology, 2017, 38, 257-263.	1.2	74
111	Understanding microstructure of the brain by comparison of neurite orientation dispersion and density imaging (NODDI) with transparent mouse brain. Acta Radiologica Open, 2017, 6, 205846011770381.	0.3	46
112	Neurite orientation dispersion and density imaging for evaluation of corticospinal tract in idiopathic normal pressure hydrocephalus. Japanese Journal of Radiology, 2017, 35, 25-30.	1.0	15
113	Quantitative Histological Validation of Diffusion Tensor MRI with Two-Photon Microscopy of Cleared Mouse Brain. Magnetic Resonance in Medical Sciences, 2016, 15, 416-421.	1.1	11
114	Diffusional Kurtosis Imaging in Idiopathic Normal Pressure Hydrocephalus: Correlation with Severity of Cognitive Impairment. Magnetic Resonance in Medical Sciences, 2016, 15, 316-323.	1.1	21
115	Pathways Linked to Internuclear Ophthalmoplegia on Diffusion-Tensor Imaging in a Case with Midbrain Infarction. Journal of Stroke and Cerebrovascular Diseases, 2016, 25, 2575-2579.	0.7	8
116	A strategy to optimize radiation exposure for non-contrast head CT: comparison with the Japanese diagnostic reference levels. Japanese Journal of Radiology, 2016, 34, 451-457.	1.0	7
117	Diffusion-tensor-based method for robust and practical estimation of axial and radial diffusional kurtosis. European Radiology, 2016, 26, 2559-2566.	2.3	9
118	Prospective estimation of mean axon diameter and extra-axonal space of the posterior limb of the internal capsule in patients with idiopathic normal pressure hydrocephalus before and after a lumboperitoneal shunt by using q-space diffusion MRI. European Radiology, 2016, 26, 2992-2998.	2.3	9
119	What is NODDI and what is its role in Parkinson's assessment?. Expert Review of Neurotherapeutics, 2016, 16, 241-243.	1.4	24
120	Neurite orientation dispersion and density imaging in the substantia nigra in idiopathic Parkinson disease. European Radiology, 2016, 26, 2567-2577.	2.3	100
121	Peking University - Juntendo University Joint Symposium on Brain and Skin Diseases. Juntendo Medical Journal, 2016, 62, 300-301.	0.1	1
122	See-through Brains and Diffusion Tensor MRI Clarified Fiber Connections: A Preliminary Microstructural Study in a Mouse with Callosal Agenesis. Magnetic Resonance in Medical Sciences, 2015, 14, 159-162.	1.1	8
123	Intersite Reliability of Diffusion Tensor Imaging on Two 3T Scanners. Magnetic Resonance in Medical Sciences, 2015, 14, 227-233.	1.1	11
124	Analysis of normal-appearing white matter of multiple sclerosis by tensor-based two-compartment model of water diffusion. European Radiology, 2015, 25, 1701-1707.	2.3	8
125	Assessing Blood Flow in an Intracranial Stent: A Feasibility Study of MR Angiography Using a Silent Scan after Stent-Assisted Coil Embolization for Anterior Circulation Aneurysms. American Journal of Neuroradiology, 2015, 36, 967-970.	1.2	72
126	Bone marrow lesions, subchondral bone cysts and subchondral bone attrition are associated with histological synovitis in patients with end-stage knee osteoarthritis: a cross-sectional study. Osteoarthritis and Cartilage, 2015, 23, 1858-1864.	0.6	50

#	Article	IF	CITATIONS
127	Cervical spondylosis: Evaluation of microstructural changes in spinal cord white matter and gray matter by diffusional kurtosis imaging. Magnetic Resonance Imaging, 2014, 32, 428-432.	1.0	33
128	A preliminary diffusional kurtosis imaging study of Parkinson disease: comparison with conventional diffusion tensor imaging. Neuroradiology, 2014, 56, 251-258.	1.1	94
129	Diffusional kurtosis imaging analysis in patients with hypertension. Japanese Journal of Radiology, 2014, 32, 98-104.	1.0	13
130	Multiple sclerosis: Benefits of q-space imaging in evaluation of normal-appearing and periplaque white matter. Magnetic Resonance Imaging, 2014, 32, 625-629.	1.0	15
131	Axon Diameter and Intra-Axonal Volume Fraction of the Corticospinal Tract in Idiopathic Normal Pressure Hydrocephalus Measured by Q-Space Imaging. PLoS ONE, 2014, 9, e103842.	1.1	16
132	Effects of diffusional kurtosis imaging parameters on diffusion quantification. Radiological Physics and Technology, 2013, 6, 343-348.	1.0	26
133	Relationship between cognitive impairment and white-matter alteration in Parkinson's disease with dementia: tract-based spatial statistics and tract-specific analysis. European Radiology, 2013, 23, 1946-1955.	2.3	80
134	White Matter Alteration in Metabolic Syndrome. Diabetes Care, 2013, 36, 696-700.	4.3	34
135	Diffusional kurtosis imaging of cingulate fibers in Parkinson disease: Comparison with conventional diffusion tensor imaging. Magnetic Resonance Imaging, 2013, 31, 1501-1506.	1.0	76
136	Diffusional kurtosis imaging of normal-appearing white matter in multiple sclerosis: preliminary clinical experience. Japanese Journal of Radiology, 2013, 31, 50-55.	1.0	69
137	Verbal dysflucency as a consequence of basal ganglia infarction with selective involvement of dorsolateral prefrontal fiber tract. Journal of Neurology, 2013, 260, 2427-2429.	1.8	1
138	Anterior Cingulate Abnormality as a Neural Correlate of Mismatch Negativity in Schizophrenia. Neuropsychobiology, 2013, 68, 197-204.	0.9	10
139	Automatic Extraction of the Cingulum Bundle in Diffusion Tensor Tract-specific Analysis: Feasibility Study in Parkinson's Disease with and without Dementia. Magnetic Resonance in Medical Sciences, 2013, 12, 201-213.	1.1	3
140	White Matter Alteration of the Cingulum in Parkinson Disease with and without Dementia: Evaluation by Diffusion Tensor Tract–Specific Analysis. American Journal of Neuroradiology, 2012, 33, 890-895.	1.2	86
141	Visualizing Non-Gaussian Diffusion: Clinical Application of q-Space Imaging and Diffusional Kurtosis Imaging of the Brain and Spine. Magnetic Resonance in Medical Sciences, 2012, 11, 221-233.	1.1	101
142	New diffusion metrics for spondylotic myelopathy at an early clinical stage. European Radiology, 2012, 22, 1797-1802.	2.3	63
143	Posterior hypoperfusion in parkinson's disease With and without dementia measured with arterial spin labeling MRI. Journal of Magnetic Resonance Imaging, 2011, 33, 803-807.	1.9	61
144	Utility of time-resolved three-dimensional magnetic resonance digital subtraction angiography without contrast material for assessment of intracranial dural arterio-venous fistula. Acta Radiologica, 2011, 52, 808-812.	0.5	13

#	Article	IF	CITATIONS
145	Recent Topics of Brain MRI : Arterial Spin Labeling and New Diffusion Analysis(<special) 0.78431<="" 1="" etqq1="" td="" tj=""><td>4 rgBT /O</td><td>verlock 10 Tf</td></special)>	4 rgBT /O	verlock 10 Tf